

# Poly(butylene succinate)/Twice Functionalized Organoclay Nanocomposites: Preparation, Characterization, and Properties

Guang-Xin Chen, Eung-Soo Kim, Jin-San Yoon

Department of Polymer Science and Engineering, Inha University, Incheon 402-751, Korea

Received 21 October 2004; accepted 28 January 2005

DOI 10.1002/app.22264

Published online in Wiley InterScience (www.interscience.wiley.com).

**ABSTRACT:** A new method was attempted to improve the interaction between poly(butylene succinate) (PBS) and a commercially available organoclay, Cloisite 25A (C25A), by the addition of epoxy groups to the clay. Epoxy groups were grafted to C25A by a treatment with (glycidoxypropyl)trimethoxy silane to produce twice functionalized organoclay (TFC). Tethering PBS molecules to the epoxy groups on the surface of TFC was attempted through melt compounding. The morphological structure of the composites was analyzed with X-ray diffractometry and transmission electron microscopy. The higher degree of exfoliation of the silicate

layers in PBS/TFC and the improved mechanical properties, in comparison with those of PBS/C25A, were attributed to the increased interfacial interaction between PBS and TFC. TFC accelerated the crystallization of PBS more effectively than C25A, and this indicated that TFC was more efficacious for the nucleation than C25A. © 2005 Wiley Periodicals, Inc. *J Appl Polym Sci* 98: 1727–1732, 2005

**Key words:** biodegradable; clay; modification; nanocomposites

## INTRODUCTION

Silicate-layered polymer nanocomposites have recently been the focus of both academic and industrial attention<sup>1,2</sup> because these nanocomposites often exhibit greatly enhanced physical and/or chemical properties even with much smaller amounts of silicate in comparison with conventional microscale composite materials.<sup>3–7</sup> The origin of the superior properties of the polymer/clay nanocomposite is thought to originate not only from their molecular-level dispersion of 1-nm-thick aluminosilicate layers in the polymer matrix but also from the strong interactions between the polymer matrix and the layers.<sup>8</sup> To improve the interaction between the polymer and clay, various cationic surfactants with functional groups have been used to modify the clay through an ion-exchange reaction.<sup>9</sup> Another approach for the improvement of the compatibility between the polymer and clay is the introduction of polar functional groups such as maleic anhydride to the polymer matrix. Both intercalated and exfoliated structures coexist in polypropylene

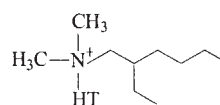
(PP)/clay composites with maleic anhydride grafted PP as an additive.<sup>10</sup> However, the window of the spectrum of the two approaches is very narrow because of the limited availability of the chemicals.

In this study, we devised a new and convenient method to introduce additional functional groups to the organoclay. We call this clay *twice functionalized organoclay* (TFC).<sup>1</sup> TFC was prepared by the reaction of (glycidoxypropyl)trimethoxy silane (GPS) with the silanol groups on Cloisite 25A (C25A). Other silane compounds can also be employed with different functional groups,<sup>11</sup> which can specially interact with the polymer to further improve the interfacial interaction. The clay–polymer hybrid thus obtained is expected to exhibit fine morphology and superior mechanical properties.

## EXPERIMENTAL

### Materials

Poly(butylene succinate) (PBS) was manufactured by IRE Chemical Co. (Seoul, South Korea) with a weight-average molecular weight of  $5 \times 10^4$ . It was dried in a vacuum oven for at least 2 days at 40°C. The organically modified clay, C25A, was purchased from Southern Clay Product, Inc. (Gonzales, TX). The structure of the organic modifier is as follows:



Correspondence to: J.-S. Yoon (jsyoon@inha.ac.kr).

Contract grant sponsor: Interdisciplinary Research Program of The Korea Science and Engineering Foundation (KOSEF); contract grant number: R01-2002-000-00146-0.

Contract grant sponsor: Brain Korea 21 Project (through a postdoctoral fellowship to G.-X.C.).

**TABLE I**  
**Tensile Properties of PBS and Its Composites with C25A and TFC**

Sample	Modulus (MPa)	Yield strength (MPa)	Elongation at break (%)
PBS	326.3	27.6	320.6
PBS/C25A2	404.2	29.8	169.0
PBS/C25A5	469.8	32.3	219.5
PBS/C25A10	609.8	25.2	20.4
PBS/TFC2	436.0	32.3	173.6
PBS/TFC5	509.5	36.7	374.4
PBS/TFC10	671.2	36.6	264.4

where HT is hydrogenated tallow (~65% C18, ~30% C16, and ~5% C14).

The silane coupling agent GPS was supplied by Aldrich (St. Louis, MO).

### Preparation of TFC

After GPS (3.5 g) was hydrolyzed at pH 4.0 for 4 h with acetic acid in an ethanol (90 wt %)/deionized water (10 wt %) mixture (200 mL), C25A (10 g) was added, and then the mixture was heated with refluxing at 70°C for 12 h. The product was diluted with *n*-propanol five times to remove the soluble homocondensates and then filtered and repeatedly washed with ethanol at room temperature. The product was dried in a vacuum oven at 40°C for at least 48 h. The grafted amount of epoxy was 0.359 mmol/g, which was determined with the chemical titration method.<sup>1,7</sup>

### Preparation of the composites

Composites of PBS and clay were prepared by the melt compounding of PBS with the clays at 140°C for 6 min. A detailed description can be found in our previous article.<sup>7</sup> The compositions and characteristic parameters of PBS and its composites are presented in Table I.

### Measurements

X-ray measurements were carried out with a Philips PW1847 X-ray diffractometer (Almelo, The Netherlands) with reflection geometry and Cu K $\alpha$  radiation (wavelength = 1.54 Å) operated at 40 kV and 100 mA. Data were collected within the range of scattering angles ( $2\theta$ ) of 2–10°.

Transmission electron microscopy (TEM) images were obtained with a TEM 2000 EX-II instrument (JEOL, Tokyo, Japan) operated at an accelerating voltage of 100 kV to observe the nanoscale structures of the various nanocomposites. All the ultrathin sections (<100 nm) were microtomed with a Super Nova 655001 instrument (Leica, Switzerland) with a dia-

mond knife and were then subjected to TEM observation without staining.

To observe the effect of clay incorporation on the crystallinity of PBS, differential scanning calorimetry (DSC) experiments were performed with a PerkinElmer DSC 7 series instrument (Wellesley, MA) under a constant nitrogen flow at a heating rate of 20°C/min. The sample weight was maintained at ~5 mg for all the measurements, and each reported result is an average of three replicates. The temperature and heat of fusion were calibrated with an indium standard.

Dynamic mechanical analysis of neat PBS and its composites was measured with a Q800 (TA Instruments, New Castle, DE) in the bending mode. The temperature dependence of the dynamic storage modulus ( $E'$ ) and loss modulus and their ratio ( $\tan \delta$ ) was determined at a constant frequency ( $\omega$ ) of 3.5 rad/s, at a strain amplitude of 0.05%, and in the temperature range of –60 to +100°C at 2°C/min.

Tensile specimens were prepared from hot-pressed sheets of PBS, PBS/C25A, and PBS/TFC. The specimens were subjected to uniaxial elongation at room temperature. All the measurements were carried out with a Hounsfield universal testing machine at a crosshead speed of 50 mm/min.

## RESULTS AND DISCUSSION

### Structure and morphology of the composites

Figure 1 shows X-ray diffractometry (XRD) patterns corresponding to C25A, TFC, and PBS/C25A and PBS/TFC composites. The number following the abbreviation is the weight percentage of the clay. For example, PBS/C25A2 is the composite composed of 98 wt % PBS and 2 wt % C25A.

The interlayer spacing of the clays was increased and the XRD peak shifted toward a lower angle because of intercalation by the polymer molecules. The interlayer spacing of  $d(001)$  of C25A and TFC was 18.5 and 18.6 Å, respectively. The  $d$ -spacing between the layers was 27.1 and 27.6 Å for PBS/C25A10 and PBS/TFC10, respectively. The intensity of the  $d(001)$  peak became weaker and slightly shifted toward a lower diffraction angle as the content of clay in the PBS/clay composite decreased; that is, for PBS/C25A5, the  $d_{001}$  spacing was 27.4 Å, whereas for PBS/C25A2, it was 27.5 Å. The same trend was observed for PBS/TFC composites, and the interlayer spacing of PBS/TFC composites increased from 27.5 to 27.7 Å as the concentration of TFC decreased from 5 to 2 wt %. The increase in the  $d$ -spacing of the composites, compared with that of the corresponding pristine organoclay, indicates that lots of PBS molecules were inserted into the interlayer space of the organoclay.

As can be seen from the XRD data, the  $d$ -spacing of the clay in the composite was almost the same

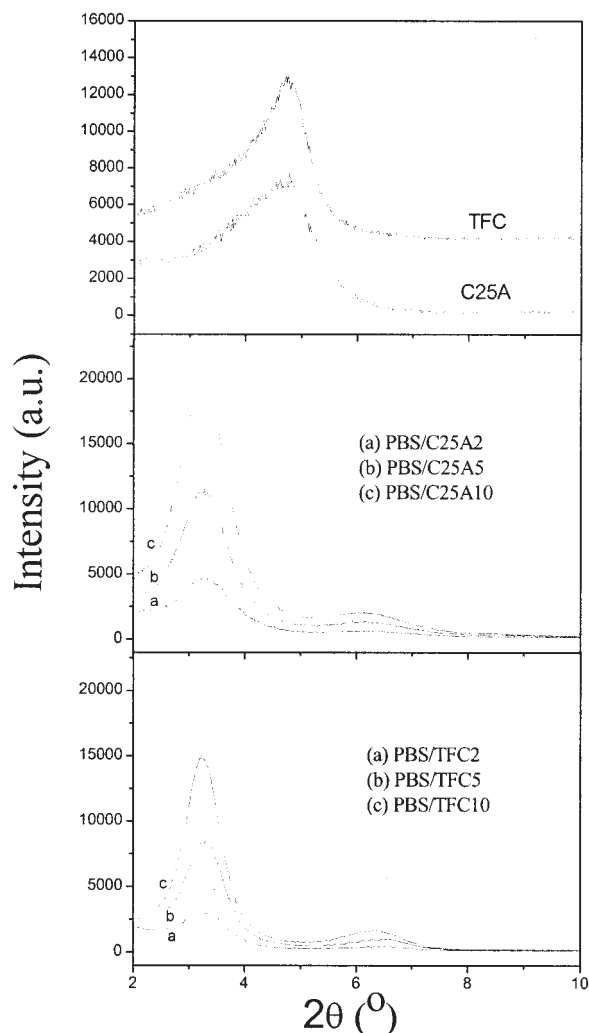


**Figure 1** X-ray diffraction patterns of C25A, TFC, and PBS composites with the two clays.

whether C25A or TFC was used. However, the peak intensity from PBS/TFC was much more attenuated than that from PBS/C25A. The decreased intensity of the peak was attributed to partial disruption of parallel stacking or layer registry of TFC, which gave rise to some exfoliation of the clay platelets. The intercalation/exfoliation coexistence in the PBS/TFC composite was further confirmed through TEM images, as shown in Figure 2, in which a typical TEM micrograph of the composite with 5 wt % C25A is compared with that of the composite with 5 wt % TFC.

Nanometer-range intercalated clay tactoids can be clearly seen in Figure 2(b) for the PBS/C25A composite. The dark lines correspond to a cross section of the clay sheets approximately 1 nm thick, and the gap between two adjacent lines is the interlayer spacing or gallery. The measured distance between the two adjacent lines, that is, the interlayer spacing of intercalated tactoids, obtained from the TEM results, is consistent with those from the XRD data. In contrast, the TEM image of PBS/TFC in Figure 2(a) exhibits individual layers as well as stacks of the silicate layers. Therefore, it can be said that a higher degree of exfoliation of the silicate layers was obtained in the case of the PBS/TFC composite in comparison with that of the PBS/C25A one, even though the X-ray diffraction pattern of the neat TFC was almost identical to that of the neat C25A.

**Thermal analyses of the PBS/clay composites**

DSC experiments were performed for PBS, PBS/C25A, and PBS/TFC. The variation of the heat of fusion with different clay compositions is shown in Figure 3. The heat of fusion went down as the clay content increased whether C25A or TFC was used; this

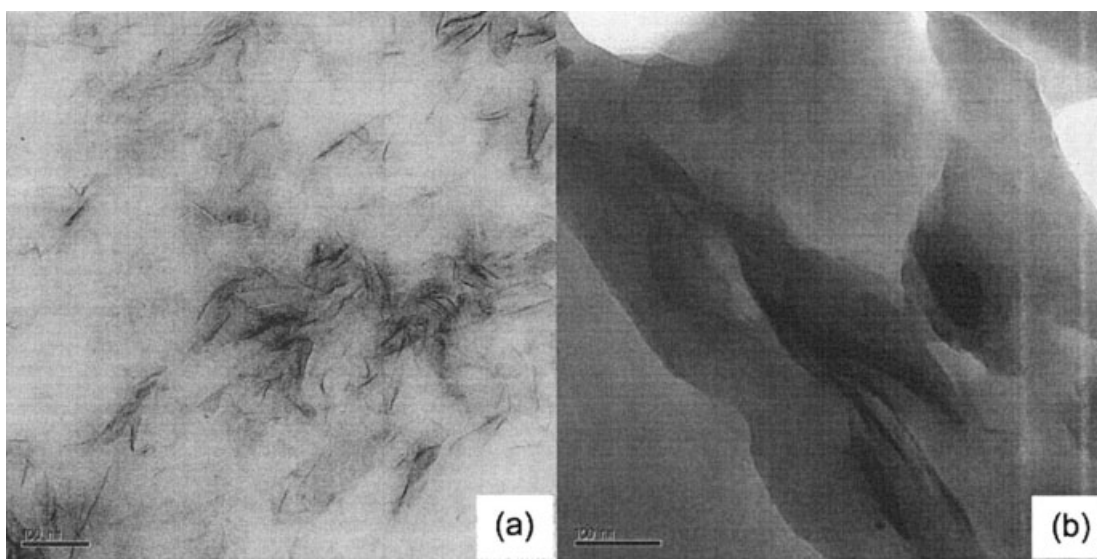


**Figure 2** TEM images of PBS composites with the two clays: (a) PBS/TFC and (b) PBS/C25A. The clay concentration was 5 wt %.

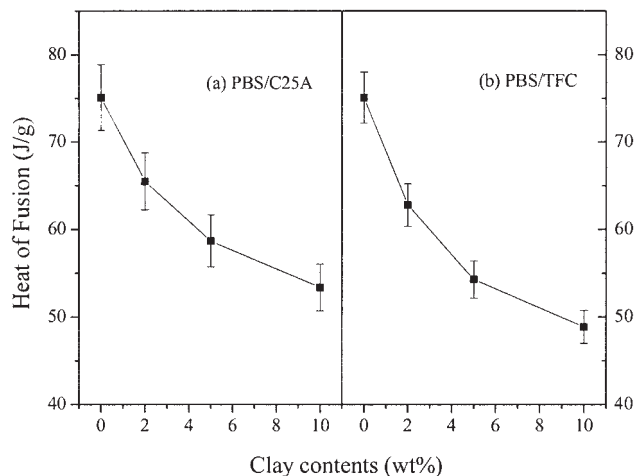


**Figure 3** Heat of fusion of PBS/clay composites at different clay loadings. An average of three replicates was taken. The error bars represent the spread of the three measurements.

indicated that the incorporation of the organic substances reduced the crystallinity of PBS. The decrease in the crystallinity was more pronounced when TFC rather than C25A was incorporated, as demonstrated in Figure 3(b). This is because the aluminosilicate layers were dispersed to a higher degree in the TFC-containing composite than those in the C25A-containing one. The higher degree of dispersion indicates more favorable interaction between TFC and PBS than between C25A and PBS, which consequently hinders the mobility of the polymer chains to a greater degree. However, the melting peak temperature ( $T_m$ ) of the composites was  $112.02 \pm 0.3^\circ\text{C}$ , being independent of the clay loading; this means that the crystalline lamellar thickness was almost the same.

Figure 4 exhibits DSC curves of the composites obtained during cooling at  $20^\circ\text{C}/\text{min}$  from the molten state. The crystallization temperature went up as the concentration of the clays increased. Therefore, the introduction of the clays sped up the crystallization, and this means that the clays acted as nucleating agents for the crystallization.

TFC was more effective for the nucleation than C25A because TFC was more uniformly dispersed in the PBS matrix than C25A, as demonstrated in Figure 2.

Further research is needed to find rationales for the reason that the heat of fusion goes down as a result of the introduction of TFC, even though TFC accelerates the crystallization of PBS and  $T_m$  remains almost the same, regardless of the TFC content.

### Dynamic viscoelastic properties of the nanocomposites

Figure 5 shows the temperature dependence of  $E'$  and  $\tan \delta$  for neat PBS and its composites with C25A and

TFC in the range of  $-60$  to  $100^\circ\text{C}$ . The  $\tan \delta$  peak temperature was not significantly affected by the clay incorporation. Over the entire temperature range,  $E'$  of the composites was higher than that of neat PBS and increased with an increase in the clay content. However,  $E'$  reached a plateau above  $60^\circ\text{C}$  for both neat PBS and the composites. The plateau value of  $E'$  was almost the same, regardless of the clay loading. The same phenomenon was also observed in a poly(L-lactide)/clay system in which, above a certain temperature, the effect of the clay incorporation on  $E'$  became negligible and the stiffness became matrix-dependent.<sup>12</sup>

Higher  $E'$  values were achieved for PBS/TFC composites than for PBS/C25A ones because of more favorable interaction of PBS with TFC than with C25A.

A weak shoulder peak appearing at  $\sim 50^\circ\text{C}$  in the  $\tan \delta$  profile in Figure 5 was believed to come from the relaxation of PBS segments confined within the clay layers.

### Mechanical properties

Table I demonstrates the tensile properties of the composites. The yield strength of the composites increased remarkably as a result of the introduction of the clay. It increased from 27.6 to 32.3 and 36.7 MPa as the concentration of C25A and TFC, respectively, increased to 5 wt %. However, as the clay content went up to 10 wt %, the yield strength decreased to 25.2 and 36.6 MPa for C25A and TFC, respectively. The larger decrease of the yield strength for PBS/C25A, compared with that of PBS/TFC, was attributed to the larger amount of agglomeration in the former composite than in the latter one. A good dispersion to avoid agglomeration is a crucial factor for enhanced

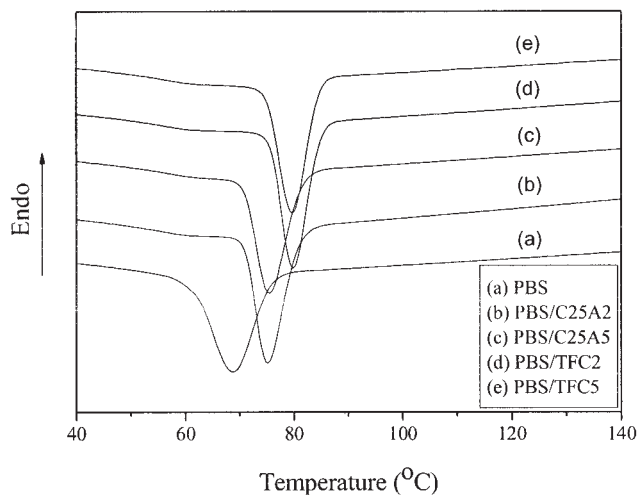


**Figure 4** DSC crystallization curves of PBS at different clay loadings.

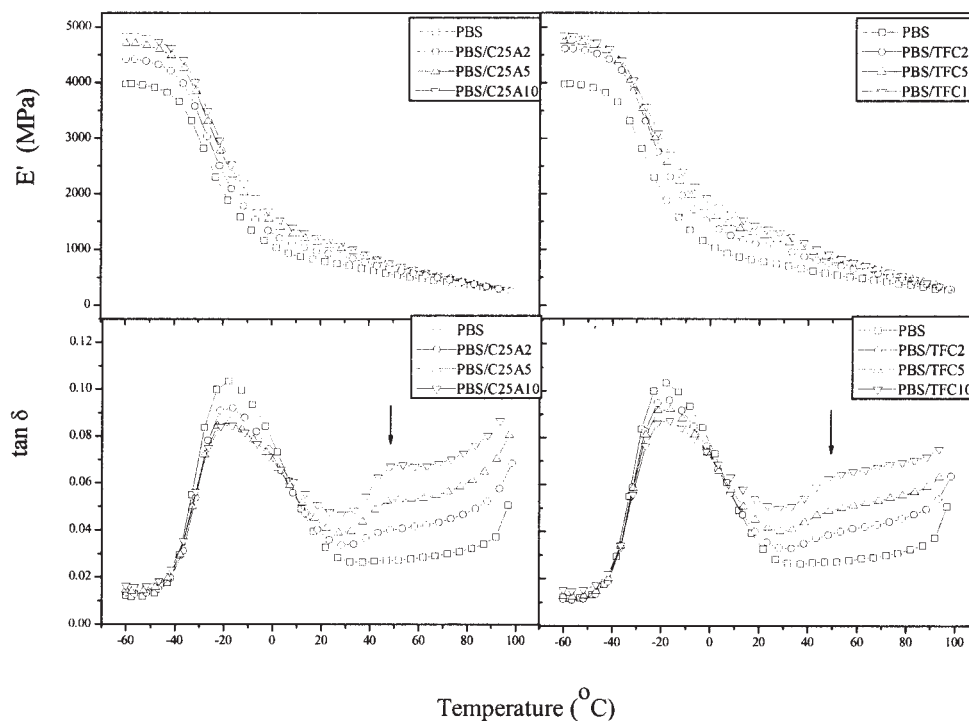


**Figure 5** Dynamic viscoelastic behavior of neat PBS and PBS composites with TFC and C25A.

mechanical properties<sup>13</sup> because cracks are usually initiated on and propagate through the agglomerates.<sup>14</sup> The tensile modulus of the PBS composites with C25A and TFC was raised from 326.3 to 609.8 and 671.2 MPa, respectively, as the concentration of the clays increased to 10 wt %.

The more significant enhancement of the yield strength and tensile modulus of the PBS/TFC composite, compared with those of PBS/C25A, was ascribed to the stronger interaction between PBS and TFC.

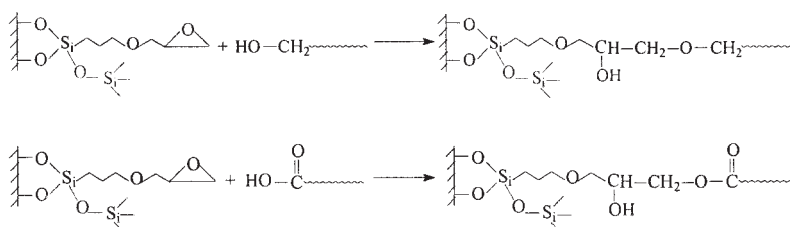
The elongation at break of the composites behaved very awkwardly, in that it went down sharply and then rose as the concentration of the clay increased to 5 wt %. A further increase in the clay concentration lowered the elongation at break.

The elongation at break of PBS/C25A with 10 wt % C25A was 20.4%, whereas that of PBS/TFC containing the same concentration of TFC was 264.4%.

The higher elongation at break, yield strength, and tensile modulus of the PBS/TFC composites, compared with those of the PBS/C25A composites, were due to a higher degree of exfoliation and promoted interaction between TFC and PBS through the potential chemical reaction. The reaction mechanism between the epoxy groups on TFC and the end-functional groups of PBS can be schematized as shown in Scheme 1.<sup>15,16</sup>

## CONCLUSIONS

A new and convenient method was devised to prepare TFC through the reaction of GPS with the hydroxy groups of organoclay C25A. TFC and C25A were melt-compounded with PBS to prepare PBS/C25A and PBS/TFC nanocomposites. The epoxy groups on the surface of TFC played a key role in the exfoliation of the clay and the improvement of the mechanical prop-



**Scheme 1**

erties. The mechanical properties of PBS were greatly improved via compounding with TFC because of the increased interfacial interaction leading to significant exfoliation of the clay platelets.

## References

1. Chen, G. X.; Choi, J. B.; Yoon, J. S. *Macromol Rapid Commun* 2005, 26, 183.
2. Ray, S. S.; Yamada, K.; Okamoto, M.; Ogami, A.; Ueda, K. *Chem Mater* 2003, 15, 1456.
3. Krikorian, V.; Pochan, D. J. *Chem Mater* 2003, 15, 4317.
4. Wang, Z. M.; Nakajima, H.; Manias, E.; Chung, T. C. *Macromolecules* 2003, 36, 8919.
5. Viville, P.; Lazzaroni, R.; Pollet, E.; Alexandre, M.; Dubois, P. *J Am Chem Soc* 2004, 126, 9007.
6. Ray, S. S.; Okamoto, K.; Okamoto, M. *Macromolecules* 2003, 36, 2355.
7. Chen, G. X.; Kim, H. A.; Shim, J. H.; Yoon, J. S. *Macromolecules* 2005, 38, 3738.
8. Kawasumi, M. *J Polym Sci Part A: Polym Chem* 2004, 42, 819.
9. Okada, O.; Kawasumi, M.; Usuki, A.; Kojima, Y.; Kurauchi, T.; Kamigaito, O. *Mater Res Soc Symp Proc* 1990, 171, 45.
10. Manias, E.; Touny, A.; Wu, L.; Strawhecker, K.; Lu, B.; Chung, T. C. *Chem Mater* 2001, 13, 3516.
11. Tesoro, G.; Wu, Y. In *Silanes and Other Coupling Agents*; Mittal, K. L., Ed.; VSP: Utrecht, The Netherlands, 1992.
12. Krikorian, V.; Pochan, D. J. *Chem Mater* 2003, 15, 4317.
13. Chang, J. H.; An, Y. U.; Cho, D.; Giannelis, E. P. *Polymer* 2003, 44, 3715.
14. Masenelli-Varlot, K.; Reynaud, E.; Vigier, G.; Varlet, J. *J Polym Sci Part B: Polym Phys* 2002, 40, 272.
15. Ju, M. J.; Chang, F. C. *Appl Polym Sci* 1999, 73, 2029.
16. Ashcroft, W. R. In *Chemistry and Technology of Epoxy Resins*; Ellis, B., Ed.; Blackie: Glasgow, United Kingdom, 1993.